Laboratory 5

Energy-Dispersive X-Ray Spectrometry

5.1 Spectrometer Setup

Experiment 5.1: Spectrum Acquisition. A typical spectrum from copper is shown in Figure A5.1. The low-energy line is the compressed *L*-series and the two higher-energy lines are the CuK_α and K_β.

Experiment 5.2: Energy Calibration Check. The CuL_α and CuK_α lines in Figure A5.1 are within one channel (10 eV or 20 eV) of their correct positions. This level of calibration is adequate for most purposes.

5.2 Beam Current and Dead Time

These experiments show how the count rate is limited in EDS systems and give some indication as to the appropriate count rate to use in various situations.

Experiment 5.3: Comparing Live Time and Real Time. Note in the table below that the real time to achieve a particular live time, or number of counts, becomes larger as the beam current increases.

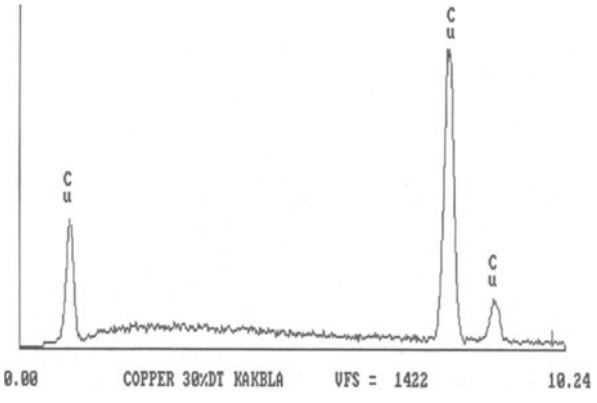

Figure A5.1. A typical spectrum from copper at a beam energy of 20 keV.

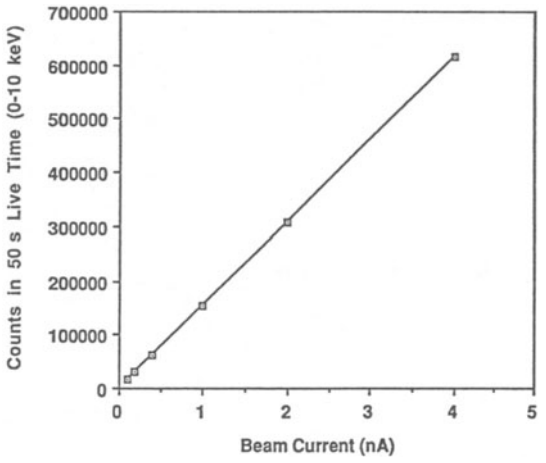

Figure A5.2. Collected x-ray counts in 50 sec live time versus beam current at 20 keV.

Dead time	Live time	Real time	Beam current
10%	30 sec	35 sec	16 pA
40%	30 sec	50 sec	254 pA
80%	30 sec	140 sec	1 nA

Experiment 5.4: Testing the Dead Time Correction Circuit. Figure A5.2 shows a linear relationship between collected counts and beam current at least up to 10,000 counts/sec.

Experiment 5.5: Maximum Output Count Rate. The counts collected per second of real time go through a maximum as shown in Figure A5.3.

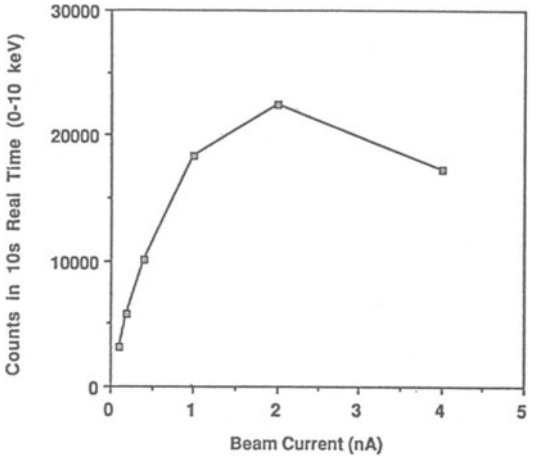

Figure A5.3. Collected counts in 10 sec real time versus beam current at 20 keV. Note that the maximum throughput of x-ray counts occurs for a beam current of about 2 nA.

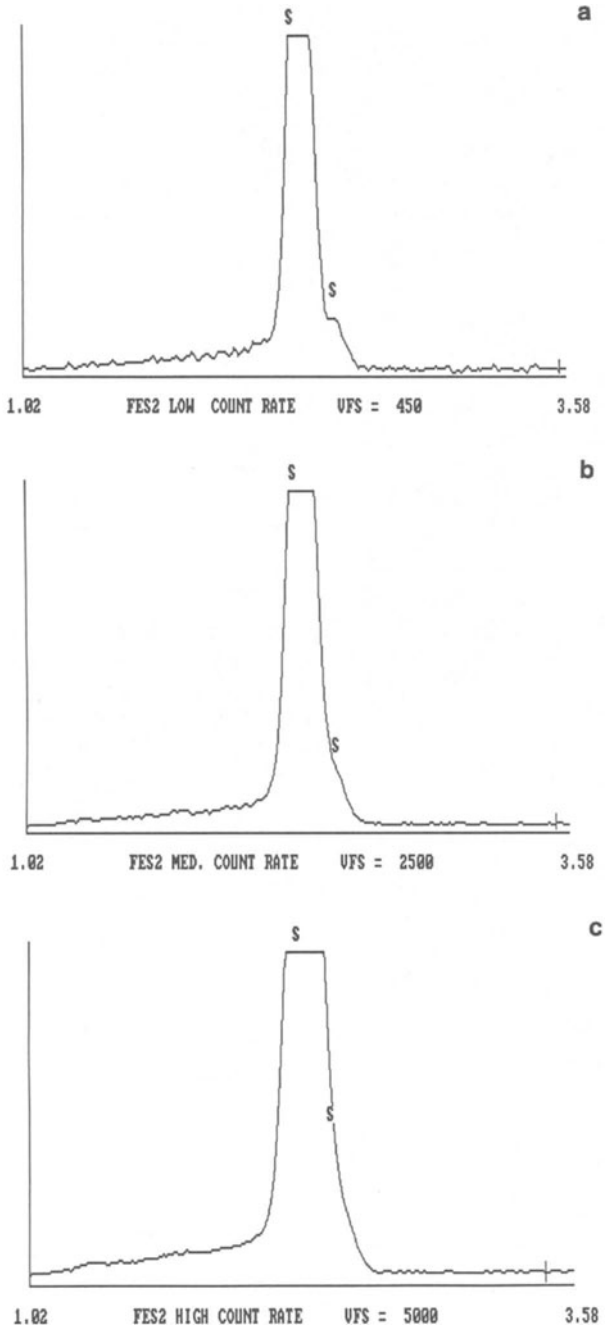

Figure A5.4. Resolution versus amplifier time constant for the sulfur K_α and K_β lines. (a) Long time constant provides some resolution of the K_β line. (b) Medium time constant. (c) Short time constant (used for high count rates) provides no resolution of K_β line.

Experiment 5.6: Detector Resolution. The degradation of resolution with increasing count rate capability is clearly shown in Figures A5.4a,b,c. The spectrum with the best resolution of the sulfur K_α and K_β (Figure A5.4a) was taken with a long amplifier time constant which limited the total number of counts processed to about one-tenth that of Figure A5.4c, in which there is no resolution of the *K*-series peaks. The setting to use depends upon the particular analyst's situation. The FWHM of the SK_α is less than the resolution value stamped on the detector dewar because the standard resolution for a detector specification is always measured at 5.9 keV.

5.3 Spectral Artifacts

Experiment 5.7: Stray Radiation. If any x-rays are excited when the probe is in the hole (e.g., platinum or aluminum), there must be some stray x-rays or electrons exciting regions far from the beam. Figure A5.5 shows an example.

Experiment 5.8: Escape Peaks, Sum Peaks, and System Peaks. Figure A5.6 shows the most common spectral artifacts. Escape peaks will always have an energy equal to the energy of the parent line minus the energy of the silicon x-ray (1.74 keV). Moreover, the magnitude of the escape peak relative to the parent peak is fixed for a particular parent line. Sum peaks are due to the simultaneous arrival of two TiK_α photons in the detector crystal creating electron-hole pairs in numbers corresponding to a single photon with the sum energy. By reducing the count rate and counting for a longer time, this artifact can be reduced to a low

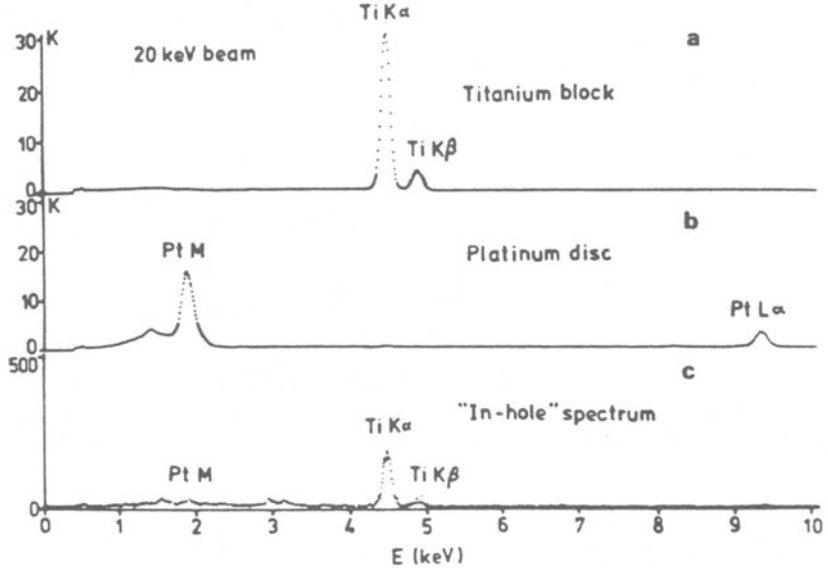

Figure A5.5. Spectra obtained from the components of a Faraday cup. (a) Titanium block directly excited by electrons. (b) Platinum disc. (c) "In-hole" spectrum.

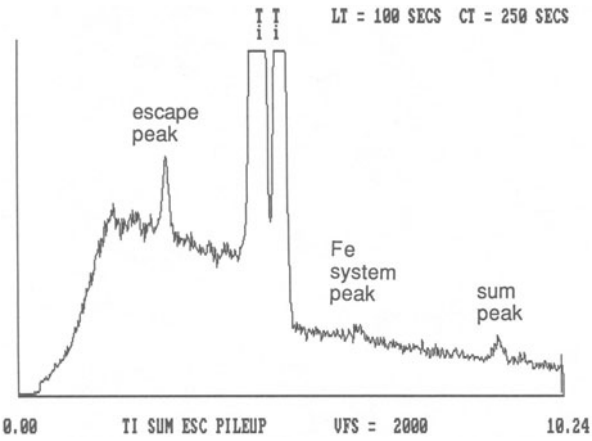

Figure A5.6. Spectrum from pure titanium showing a silicon escape peak for TiK_α, a small iron system peak generated by backscattered electrons hitting the polepiece, and a TiK_α sum peak.

level. The Fe system peak may be reduced by covering the offending parts of the specimen chamber with a low-Z element such as carbon (consult the microscope manufacturer).

Experiment 5.9: False Peaks: Figures A5.7a,b show the danger of not taking enough counts and trying to smooth the spectrum mathematically. Random background counts can look like small peaks after a smoothing operation. In general, smoothing is an unnecessary and potentially misleading operation. If one feels compelled to have a spectrum with a smooth background, don't smooth--take more counts!

Experiment 5.10: Pulse Pileup. Magnesium pulses may be so close to the noise level that the discriminator cannot reject them. This allows a pulse pile-up continuum to build up just below the MgK_α sum peak.

Experiment 5.11: Pile-up Correction Failure. The counts lost from the peak which appear in the pile-up continuum represent a failure in the pile-up correction which arises from a fundamental limitation in the circuitry. Around the energy of MgK (1.25 keV), the pulse heights delivered by the fast channel are falling into the electronic noise, thus defeating the efforts of the circuits to make an accurate pile-up correction. For peaks with energies below 1.25 keV, there is no pile-up rejection, so these peaks should be acquired at low count rates. This phenomenon has serious implications for quantitative analysis of light elements, and is one more reason that quantitative light element analysis should be carried out with wavelength-dispersive spectrometry.

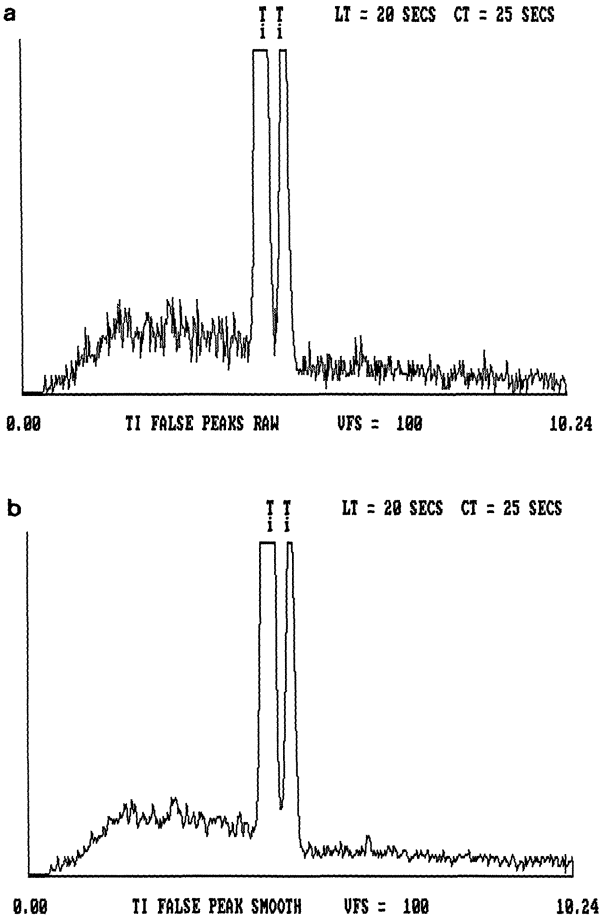

Figure A5.7. Spectrum containing insufficient counts collected over too short a time. (a) Raw unsmoothed spectrum. (b) Mathematical smoothing of spectrum (a). Small apparent peaks arise that are not present in Figure A5.6. (Note also that the sum peak of Figure A5.6 is completely absent while there is evidence for the escape peak and the iron system peak.)

Experiment 5.12: Incomplete Charge Collection. The shape of the CuK_α peak is nearly an ideal gaussian, whereas the K_α peak typically shows a slightly higher tail on the low-energy side. If your MCA can generate a gaussian peak for the K_α, assess the deviation from the ideal gaussian.

Laboratory 6

Energy-Dispersive X-Ray Microanalysis

6.1 Families of X-Ray Spectra

With increasing atomic number each x-ray family tends to spread out revealing individual lines that were unresolved for lower-Z elements.

Experiment 6.1*: *K, L, and M Spectra. For the lighter elements ($Z < 26$) only a K series (unresolved for $Z < 16$) is detected with a Be window detector. The aluminum spectrum in Figure A6.1a shows a single peak containing the unresolved K_α and K_β lines). Copper will exhibit an L peak in which the three main L lines are not resolved (see Figure A6.1b). For heavier elements, the L series is more widely spaced in energy such that the separate L_α, L_β, L_γ peaks are resolved (see the gold spectrum in Figure A6.1c). Note the weak peak on the low-energy side of the L_α, the Ll. For the heaviest elements a single strong M line (with weak M lines on either side) can be observed in addition to the L-series (see Figure A6.1d). It is important to be aware of the weak lines that accompany the L and M series so that they will not be identified as another element.

Experiments 6.2: K Family X-Rays. These spectra show how the K spectra appear for elements of increasing atomic number. The lines spread out and are resolved for the heavier elements. For Ti, Fe, and Cu, note the presence of well-resolved K_α and K_β peaks with an approximate peak height ratio of 10:1. Note the difference in the appearance of the K family for Al, Si, and S. The K_β peak is not resolved for Al, and it only forms a slight distortion on the high-energy side of the K_α peak for Si. For sulfur, the K_β forms a significant distortion on the high energy side of the K_α peak but is not completely resolved.

Experiment 6.3: L Family X-Rays. For Cu, only one peak is observed. For Zr, the single peak is slightly distorted on the high-energy side. For Ag the existence of several L peaks can be observed. For Ba, all of the significant L-family lines are resolved. For Au, the lines are completely resolved, and the complexity of the L family for high-atomic-number elements is well-illustrated.

Experiment 6.4: M Family X-Rays. For Ta, only one slightly distorted peak is observed. For Au and Pb, the unresolved M_α and M_β peaks produce a distinctly asymmetric peak. Finally, for uranium, the separation of M_α and M_β is sufficient to observe them as separate peaks.

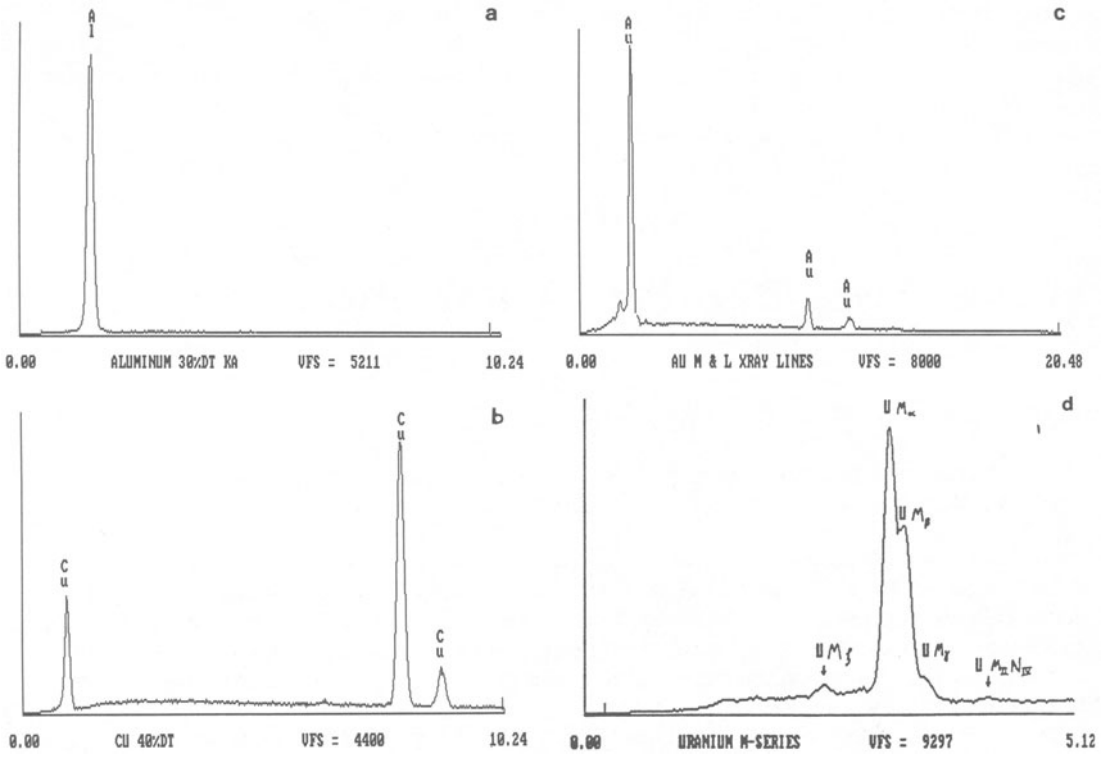

Figure A6.1. Examples of *K*, *L*, and *M* spectral families for selected elements. (a) Aluminum; (b) copper; (c) gold; (d) uranium.

6.2 Qualitative Analysis

Experiment 6.5: Qualitative Analysis of a Simple Spectrum. Figure A6.2 shows an EDS x-ray spectrum containing four peaks. Using the qualitative analysis guidelines, we start with the highest energy peaks. In this case, the *K* family of iron is recognized by the K_α peak (6.40 keV) and the K_β peak (7.05 keV) at about 10% of the K_α intensity. Next we look for the *L* series for Fe (0.70 keV). While there is a peak at about 0.55 keV, no peak is apparent at 0.70 keV. There is a slight bump in the background at 4.65 keV which is the Si escape peak for Fe K_α (6.40 keV - 1.74 keV = 4.66 keV). Next we analyze the largest peak in the spectrum at 2.30 keV. This peak could either be the sulfur K_α line, the molybdenum L_α line, or the lead M_α line. This peak is very strong and is not associated with other weaker peaks; therefore, it must be the unresolved sulfur $K_{\alpha,\beta}$ pair. If small amounts of Mo or Pb were present in this specimen they could not be identified without examining higher energy lines in the 10-20 keV range. The small peak at 0.55 keV can be recognized as the Si escape peak for sulfur K_α (2.30 keV - 1.74 keV = 0.56 keV). Thus the specimen contains only iron and sulfur (FeS_2).

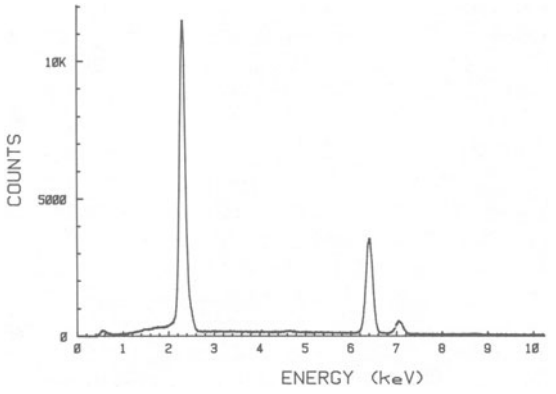

Figure A6.2. Simple spectrum for qualitative analysis. Specimen is iron pyrite (FeS_2).

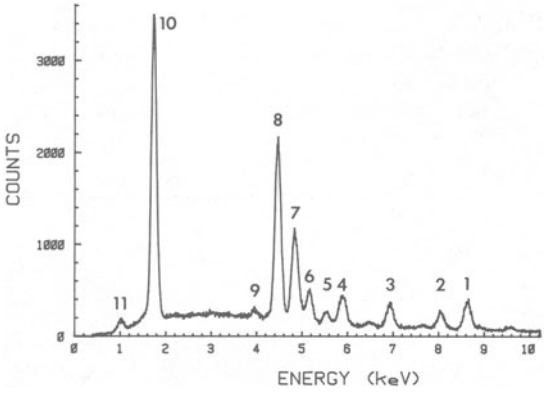

Figure A6.3. Complex spectrum for qualitative analysis. Specimen is a glass containing many dissolved metal atoms. Peaks are numbered for identification in Table A6.1.

Table A6.1. Analysis of a Complex Spectrum

Peak No.	Measured Energy	Identification (Energy)	Remarks
1	8.62 keV	ZnK_α (8.63 keV)	K_β found at 9.58 keV
2	8.04 keV	CuK_α (8.04 keV)	K_β found at 8.90 keV
3	6.92 keV	CoK_α (6.93 keV)	K_β found at 7.62 keV
4	5.90 keV	MnK_α (5.90 keV)	K_β found at 6.50 keV
5	5.54 keV	BaL_γ (5.53 keV)	small peak difficult to identify by itself
6	5.18 keV	Ba$L_{\beta 2}$ (5.16 keV)	
7	4.84 keV	Ba$L_{\beta 1}$ (4.83 keV)	
8	4.46 keV	BaL_α (4.47 keV)	
9	3.96 keV	BaLl (3.95 keV)	
10	1.74 keV	SiK (1.74 keV)	K_β not resolved
11	1.04 keV	NaK (1.04 keV)	K_β not resolved

Experiment 6.6: Qualitative Analysis of a Complex Spectrum. Figure A6.3 shows a spectrum containing at least 10 recognizable peaks. Again working from high energy to low energy for the large peaks, we note the energies of these peaks in Table A6.1.

There are two approaches to this spectrum. Starting at the highest energy peak, which is several times the background intensity (peak 1), we can identify this as ZnK_α both by energy and by the fact there is a small peak at the appropriate energy for ZnK_β. Peaks 2, 3, and 4 may be identified in a smiliar manner. Peak 5 is more than 130 eV away from the nearest K_α line, whereas peaks 1-4 could be identified to within about 30 eV. Since peak 5 is not near a K_β peak and is at an energy too high to be an M line, it may be part of an *L*-series (skip this peak for now). Peak 6 is also more than 100 eV away from any *K*-line (skip this peak also). Peaks 7 and 8 can be identified as the BaL_β and L_α peaks, respectively. At this point it is obvious that peaks 5, 6, and 9 are the BaL_α, Ba$L_{\beta 2}$, and Ba*Ll*, respectively. Peaks 10 and 11 can be identified as the Si*K* and Na*K* peaks for which the K_β lines are not resolved.

Experiment 6.7: Automatic Qualitative Analysis. It should be clear from a comparison of your manual peak identification with the elements identified by the automatic peak search that caution is always necessary with such automatic routines. In cases where the automatic search yields ambiguous results the manual methods must still be used. When the peaks are too small or the spectrum too noisy, the automatic search may fail to recognize a peak. In the worst case, the data file could even be damaged, leading to incorrect identifications. The value of experience, intuition, and common sense in the analysis of spectra cannot be overemphasized.

6.3 Quantitative Analysis

Experiment 6.8: Establishing Proper Working Conditions. The new copper spectrum should have the same shape as the library standard Cu spectrum although the relative intensity may be slightly different. The quantitative software will scale the new spectrum vertically to match the stored spectrum. Any large deviations in calibration or peak shape may cause difficulty in peak stripping and background subtraction.

Experiment 6.9: ZAF versus Standardless. Table A6.2 below shows a comparison of the ZAF and standardless output.

Table A6.2. Comparison of ZAF and Standardless Methods

Method	Line	*K* ratio	[*Z*]	[*A*]	[*F*]	At.%	Wt.%
ZAF	NiK_α	0.6700	1.025	1.001	1.000	51.05	68.70
	Al*K*	0.1277	0.970	2.447	1.000	48. 95	30.28
						100.00	98.98
Stand-	NiK_α	0.6760				50.85	69.24
ardless	Al*K*	0.1240				49.15	30.76
						100.00	100.00

As expected, the largest ZAF correction factor is the absorption correction for aluminum. The two elements emit x-rays of widely different energy so the fluorescence correction factor is negligible. There is nothing significant about the fact that the concentrations of the elements add up to 100%. In fact, if they do, it may indicate that the measurements are not independent. The precision can only be assessed by knowing the total number of counts accumulated in the peaks. Thus, the precision implied by the four significant figures may not be justified. This particular standardless routine uses the stored library spectra for pure Ni and Al to produce a K ratio, and then uses the ZAF program to calculate compositions. This works well as long as the library spectra and the unknown spectrum were taken under identical conditions.

Experiment 6.10: Effect of Take-off Angle. A small change in take-off angle due to a different specimen tilt can result in significant error if the absorption correction is large as it is in Ni-Al. Table A6.3 shows the magnitude of this effect.

Table A6.3. Effect of Take-Off Angle Changes on Composition

Take-off angle	Element	K ratio	$[Z]$	$[A]$	$[F]$	At.%	Wt.%
30°	NiK_α	0.640	1.027	1.001	1.000	46.96	65.83
	AlK	0.122	0.970	2.893	1.000	53.04	34.17
40°	NiK_α	0.677	1.024	1.001	1.000	51.06	69.42
	AlK	0.123	0.968	2.571	1.000	48.94	30.58
50°	NiK_α	0.701	1.022	1.001	1.000	53.76	71.67
	AlK	0.124	0.967	2.369	1.000	46.24	28.33

Note that the change in take-off angle from 30° to 50° causes a 17% change (error) in Al wt% composition. Since the microprobe used did not allow specimen tilting, the above results were generated by changing the take-off angle in the ZAF program.

Experiment 6.11: Effect of Beam Energy. Both ZAF and standardless programs will give inaccurate results if the voltage used in the calculation is not the same as the voltage used in taking the data. In fact, it is possible for the actual accelerating voltage to be in error by several hundred volts without the operator being aware of it. But the effects of voltage differences are most serious in standardless analysis, where library spectra taken at a different voltage will produce results that are seriously in error. For example, a standardless analysis calculated using 15 kV when the data was taken at 20 kV yields 82.86 wt% Ni instead of 69.24 wt% Ni (Table A6.2). This is an error of nearly 20%! Spatial resolution and element excitation considerations often dictate an accelerating voltage other than 20 kV, rendering the library spectra and the resultant standardless analysis useless.

References

[1] C. E. Fiori and D. E. Newbury, *Scanning Electron Microscopy/1978*, vol. I, SEM Inc., AMF O'Hare, IL, p. 401.

[2] J. A. Bearden, "X-Ray Wavelengths and X-Ray Atomic Energy Levels," NSRDS-NBS 14, National Bureau of Standards, Washington (1967). Also published in recent editions of the *CRC Handbook of Chemistry and Physics*, The Chemical Rubber Company, Cleveland, Ohio.